Simultaneous in vivo imaging of dual targets of tumor: detection and quantification with dual nano probes and computed tomography

Young Joo Suh

Department of Medicine

The Graduate School, Yonsei University

Simultaneous in vivo imaging of dual targets of tumor: detection and quantification with dual nano probes and computed tomography

Directed by Professor Jin Hur

The Doctoral Dissertation
submitted to the Department of Medicine,
the Graduate School of Yonsei University
in partial fulfillment of the requirements for the degree
of Doctor of Philosophy

Young Joo Suh

December 2015

This certifies that the Doctoral Dissertation of Young Joo Suh is approved.

Thesis Supervisor : Jin Hur

Thesis Committee Member#1 : Yong-Min Huh

Thesis Committee Member#2 : Jongduck Baek

Thesis Committee Member#3: Bumsang Kim

Thesis Committee Member#4: Byoung Wook Choi

The Graduate School
Yonsei University

December 2015

ACKNOWLEDGEMENTS

I acknowledge my deep gratitude to Professor Jin Hur, who is my thesis director, for supporting my efforts with total commitment and facilitating every step of the process. My appreciation for his guidance and encouragement is tremendous. I am also indebted to Professor Byoung Wook Choi, Yong-Min Huh, Jongduck Baek and Bumsang Kim for their help for pertinent advice to assure the superior quality of this paper.

<TABLE OF CONTENTS>

LIST OF FIGURES

ABSTRACT

Simultaneous in vivo imaging of dual targets of tumor: detection and quantification with dual nano probes and computed tomography

Young Joo Suh

Department of Medicine
The Graduate School, Yonsei University

(Directed by Professor Jin Hur)

Background: Use of multiple target-specific agents to determine disease markers and eventually make a correct diagnosis has been a standard practice in clinical medicine. We aimed to investigate the feasibility of simultaneous in vivo imaging of dual tumor targets by micro-CT imaging.

Materials and Methods: Gold nanoparticles (AuNp, 30 nm) were coated with polyethylene glycol and conjugated with anti-human epidermal growth factor receptor (HER2/neu) aptamers. Liposomes containing iodine (Lipo-I) with or without conjugation with vascular endothelial growth factor-2 (VEGFR2) aptamers were prepared. A female BALB/c-nude mouse xenograft tumor model that highly expresses the HER2/neu cancer markers was generated. Animals were divided into six groups according to the combination of contrast agents (n=3 for each group). After intravenous injection of the nanoparticle contrast agents, CT density was measured within the tumor and compared between subgroups with different kinds of contrast injection. CT-derived contrast enhancements were compared with histologic analysis by hematoxylin and eosin (H&E) and immunohistochemical (IHC) staining.

Results: The contrast enhancement of tumor was greater in the HER2-aptamer conjugated gold nanoparticle (HER2-Apt-AuNp) group than in the AuNp group immediately (39.4 vs. 7 HU), 24 hours (138.1 vs. 116.6 HU), and 48 hours

(186.0 vs. 162.4 HU) after contrast administration. The Herceptin block + HER2-Apt-AuNp group showed less enhancement (129.2 HU after 48 hours) than the HER2-Apt-AuNp group and AuNp group. The VEGFR2-conjugated liposomal iodine (VEGFR-Apt-Lipo-I) group demonstrated greater enhancement than the Lipo-I group after contrast administration (65.4 vs. 51.8 HU immediately after contrast administration). The combination of VEGFR-Apt-Lipo-I and HER2-Apt-AuNp showed greater contrast enhancement than the HER2-Apt-AuNp at 24 hours (187.4 vs. 138.1 HU) and 48 hours (208.5 vs. 186 HU), respectively. IHC staining revealed that the contrast enhancement area by AuNp and Lipo-I was largely consistent with the HER2-postive and VEGFR2-positive area, respectively.

Conclusion: Micro-CT can be applied for simultaneous in vivo imaging of dual tumor targets.

Key words: computed tomography, targeted imaging, dual contrast nan oprobe

Simultaneous in vivo imaging of dual targets of tumor: detection and quantification with dual nano probes and computed tomography

Young Joo Suh

Department of Medicine
The Graduate School, Yonsei University

(Directed by Professor Jin Hur)

I. INTRODUCTION

Use of multiple target-specific agents to determine disease markers and eventually make a correct diagnosis has been a standard practice in clinical medicine, especially in pathologic immunohistochemistry (IHC). The application of a multiple surrogate marker approach by IHC requires that tumor tissue be divided into multiple samples, each of which can then be tested in parallel with one or multiple antibodies with different optical reporters. However, obtaining multiple tumor tissue samples requires invasive procedures, which may increase the risk to the patient. Current improvements in molecular imaging technology are providing alternative noninvasive approaches to accurately reveal disease status using the same target-specific components as IHC. Imaging technology permits analysis of disease status at the level of the entire body, the lesion, and the cell, and minimizes sampling error while permitting simultaneous analysis of multiple disease factors.

For simultaneous multitargeted imaging, optical molecular imaging is a rapidly advancing imaging modality that allows simultaneous detection of multiple disease targets in preclinical studies using near-infrared dye[1] or photoacoustic imaging.[2] In contrast, pre-existing imaging modalities such as magnetic resonance imaging require multiple examinations for simultaneous multitargeting imaging. However, optical imaging has limited signal penetration

and therefore has limited applications in human body imaging.

Computed tomography (CT) has the advantage that it can be applied to human body imaging and also can acquire multitargeted images with a single scan. Nanoparticle contrast agents are essential for preclinical CT studies because conventional contrast agents are cleared from the bloodstream too quickly for effective imaging. The utility of these nanoparticle contrast agents in preclinical CT imaging has been well established.[3-8] Although these approaches are able to improve some aspects of CT imaging, development of various contrast agents for targeted CT imaging with high imaging sensitivity is still a challenge. Data in the literature have shown that targeted CT imaging of tumors in vitro and in vivo can be achieved by conjugating targeting ligands onto the surface of gold nanoparticles (AuNps).[9-13] Recently, investigators have developed a targeted CT contrast agent to visualize and quantify targets within the tumor.[7,14] We therefore hypothesized that we could detect and differentiate two CT densities from two different targeting nanoprobes using CT. The purpose of our study was to investigate the feasibility of simultaneous in vivo imaging of dual tumor targets by micro-CT imaging.

II. MATERIALS AND METHODS

1. Selection of two important targets and two different contrast materials

We searched the literature and selected two optimal targeting ligands for the breast cancer model: human epidermal growth factor receptor-2 (HER2/neu) as a growth factor marker and vascular endothelial growth factor receptor-2 (VEGFR2) as an angiogenesis marker. We selected AuNp and liposomal iodine (Lipo-I) as contrast materials. The HER2 aptamer and VEGFR2 apatmer were selected as targeting materials.

2. Synthesis of imaging nanoprobes

A. Gold nanoparticles and HER2 aptamer-conjugated gold nanoparticles

We prepared 30-nm AuNps as described previously.[15] To synthesize HER2 aptamer-conjugated AuNp (HER2-Apt-AuNp), 5 mL of sodium citrate solution (1 wt %) was added to 100 mL of deionized water (DW) in a 250-mL beaker on a hot plate. The solution was heated to boiling point, and then 1 mL of $HAuCl_4$ solution (1 wt %) was added quickly to the boiling solution. The solution was stirred for 2 hours until its color changed from transparent to a red-wine color. To conjugate HER2 aptamer with AuNp, EDC (2.9 μmol), Sulfo-NHS (2.5 μmol), and 50 μg of Apt-HER2 were added to 2 mL of AuNp (220 mg/2 mL). Side products of this reaction were removed by centrifugation at 15,000 rpm for 30 min and the product was re-dispersed in 4 mL of PBS.

.

B. Liposomal iodine nanoparticles and VEGFR aptamer-conjugated liposomal iodine nanoparticles

Lipo-I was prepared as follows: 1 g of HPC was dissolved in 1 mL of methanol and the solution was heated to 65°C. One milliliter of Visipaque 320 (iodixanol 320 mg/ml, GE Healthcare Buchler, Braunschweig, Germany) was added to the solution and stirred with a magnetic bar for 3 minutes, and then 20 mL of phosphate buffer saline (PBS) was added at a flow rate of 1 mL/min while homogenizing te suspension at 2,500 rpm using a homogenizer (T10 basic, IKA). Homogenization was continued for an additional 10 minutes while the temperature was brought down to room temperature. The prepared liposomes were washed by repeated dilution with PBS and centrifuged at least three times to remove unreacted materials and non-encapsulated iodine. Empty liposomes were prepared without addition of iodixanol. Their size, as determined by laser light scattering (DLS) using a BI-9000AT Digital Autocorrelator (Brookhaven Instruments), was 100 nm in diameter. To avoid leakage of the iodine, liposomes were stored at 4°C until use. VEGFR2-Aptamer was conjugated with Lipo-I to give VEGFR2-Apt-Lipo-I.

3. Characterization of targeted imaging nanoprobes

A. Inductively coupled plasma optical emission spectrometry

The Au concentration in the synthesized AuNp solution was analyzed using inductively coupled plasma optical emission spectrometry (ICP-OES).

B. Phantom study

Radiodensity calibration was carried out by imaging serial dilutions of AuNp and iodine, respectively. The concentration of AuNp solution was determined by ICP-OES and the iodine concentration was known to be 320 μg/μL. Hounsfield Unit (HU) values of AuNp and iodine solutions were obtained by micro-CT scanning to construct a standard curve. HU values of each AuNp and iodinated liposome sample were obtained and converted to Au and iodine concentration using the standard curve.

4. Animal model

The xenograft tumor model was generated by implantation of NIH3T6.7 fibroblast cells that highly express the HER2/neu cancer markers (1×10^7 cells suspended in 50 mL of saline per animal) into the proximal thigh of female BALB/c-nude mice (4-5 weeks of age).

5. Micro-CT protocol

Micro-CT was performed with a volumetric CT scanner (NFR-Polaris-G90MVC: NanoFocusRay, Iksan, Korea), a high-flux rotating anode X-ray tube with a Flat Panel Detector (1232×1120 pixels, 100 μm pixel size). Images were acquired at 65 kVp, 115 μA, and 142-millisecond per frame, for 700 views. Projections were acquired over a circular orbit of 360° with continuous rotation using a slip ring. Acquisition time of each projection was approximately 7–15 seconds. The estimated radiation dose using this image acquisition protocol was ~150 mGy. Images were reconstructed using the

volumetric cone-beam reconstruction (Feldkamp algorithm) in off-line mode. The size of reconstructed images was 1,024 × 1,024 pixels, and 512 slices were acquired. The final reconstructed data were converted to the Digital Imaging and Communications in Medicine (DICOM) format to generate 3D-rendered images using 3D-rendering software (Lucion, MeviSYS, Seoul, Korea).

6. In vivo CT imaging

Animals were divided into six groups according to the combination of contrast agents used (n=3 for each group). To demonstrate the targeting effect of conjugation with the HER2-aptamer, three AuNp groups were compared: (1) AuNp, (2) HER2-Apt-AuNp, (3) HER2-Apt-AuNp with Herceptin (Trastuzumab) block. To demonstrate the targeting effect of conjugation of a VEGFR aptamer, imaging was acquired in two additional groups with (4) Lipo-I and (5) VEGFR-Apt-Lipo-I. To investigate the effect of the simultaneous use of the two contrast agents, (6) a combination of HER2-Apt-AuNp and VEGFR-Apt-Lipo-I group were injected simultaneously. We set the injected dose for in vivo imaging as described in a previous study:[10] 2.5 μmol Au/g body weight for AuNp groups, and 4 μmol I/g body weight for Lipo-I groups. Contrast agent was injected via the distal tail vein and images were obtained before contrast administration, and at 0, 24, and 48 hours after bolus injection (Figure 1). For Herceptin block, Herceptin was injected 4 hours before contrast administration.

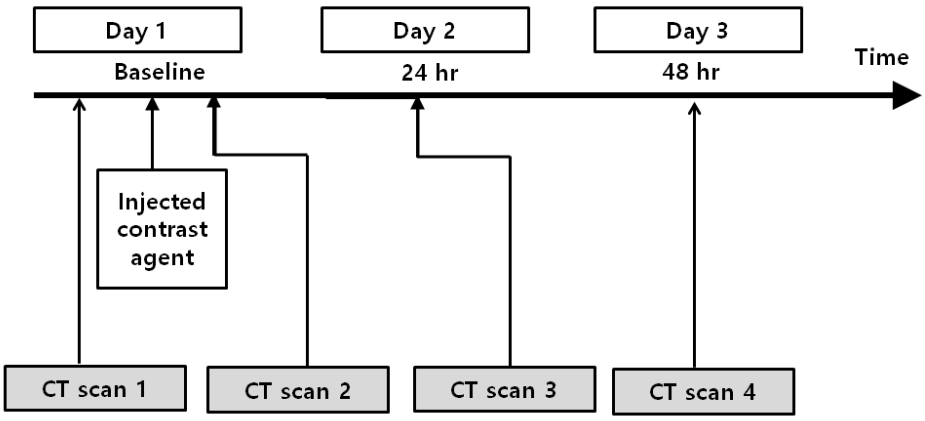

Figure 1. Flow chart of image acquisition points for in vivo micro-CT imaging. Contrast agent was injected on day 1 and scan 1 was performed just before contrast injection. CT scan 2 was performed immediately after contrast injection. CT scans 3 and 4 were performed 24 hours and 48 hours after contrast administration, respectively.

7. CT image analysis

Micro-CT images were transferred to a designated workstation for analysis (Lucion, CyberMed and Mevisys, Seoul, Korea). CT image analyses were performed by two independent observers. We drew a region of interest (ROI) on the tumor for measurement of CT density value. The ROI was first drawn for images obtained 48 hours after nanoparticle administration. Each ROI had an area greater than 15 mm^2. The ROI on the tumor was drawn to include the whole tumor and was drawn in three equidistant-placed coronal planes to cover more tumor area in total. ROIs on pre-contrast images and post-contrast images taken immediately and 24 hours after contrast administration were drawn with the same size and at the same location as the ROI for images

obtained 48 hours after contrast injection. We calculated an average density value from three different slices for each mouse. The difference in density between post-contrast (immediate, 24, and 48 hours after contrast administration) and pre-contrast densities was used as 'contrast enhancement'. The mean value for the two observers was used as a representative value. We compared contrast enhancement in the tumor between groups.

8. Histologic analysis

After CT scanning on day 2 (48 hours after contrast enhancement), the animals were sacrificed and tissues were prepared for histologic analysis. Histologic evaluation was conducted using hematoxylin and eosin (H&E) staining and IHC. Tissues were dehydrated using increasing alcohol concentrations and cleared in xylene, and then embedded in paraffin. Slices (10 μm thickness) were mounted onto glass slides and the slides were placed in a container filled with hematoxylin twice for 10 min each for nuclear staining. Tissues were rinsed in water for 10 min to remove hematoxylin, and the cytoplasm was stained with eosin and dehydrated as described above. After washing three times for 30 min, 2 or 3 drops of the mounting solution were placed on the slide and covered with a cover glass.

In addition, 10-mm thick tumor slices were prepared for IHC staining for HER2 and VEGFR2 with the following primary antibodies: rabbit anti-mouse anti-HER2 antibody (1:100; Abcam, Cambridge, United Kingdom) and rabbit anti-mouse VEGFR2 antibody (1:100; Abcam).

9. Correlation between CT results and histologic analysis

To validate CT-derived measurements (contrast enhancement), the correlation between CT images and histology was analyzed. Distribution of areas showing contrast enhancement by contrast agent was visually compared with the area showing HER2 and VEGFR2 positivity on IHC staining.

III. RESULTS

1. Characterization of contrast agent

The concentration of synthesized AuNp solution was 110.0 μg/μL Au by ICP-OES. The concentration of iodine contrast agent was known to be 320 μg/μL I. The CT density showed a linear relationship with the concentrations of AuNp and Lipo-I (Figure 2).

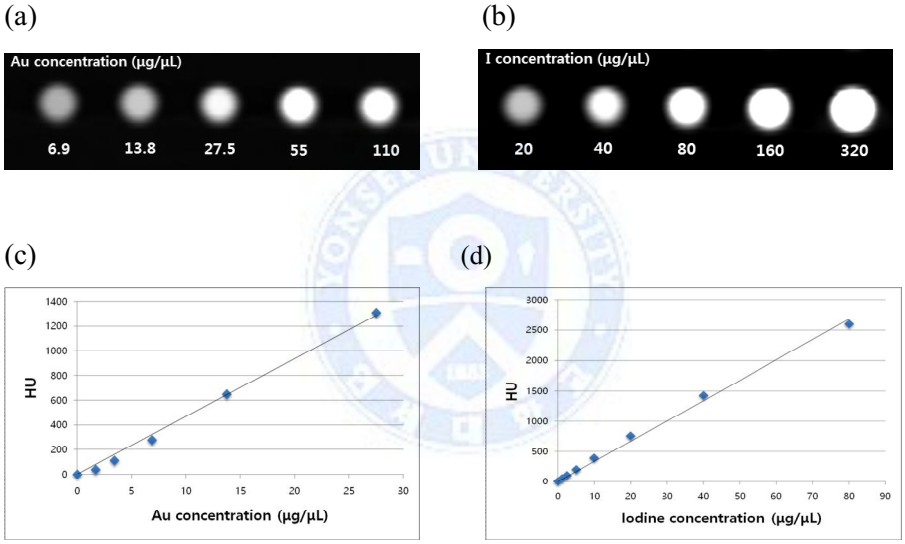

Figure 2. Phantom study results. (a, b) Computed tomography images of AuNp and Lipo-I and (c, d) plots of X-ray attenuation values at various concentrations. CT density showed a linear relationship with the concentration of AuNp and Lipo-I.

2. In vivo imaging: comparison of targeted and non-targeted contrast agent

In vivo micro-CT imaging was performed in three mice for each group. The contrast enhancement of tumor in the AuNP injection groups (AuNp, HER2-Apt-AuNp, Herceptin block with HER2-Apt-AuNp) gradually increased with increasing time (Figure 3). The contrast enhancement of the tumor was higher in the HER2-Apt-AuNp group than in the AuNp group immediately (39.4 vs. 7 HU), 24 hours (138.1 vs. 116.6 HU), and 48 hours (186.0 vs. 162.4 HU) after contrast administration (Figure 4). The Herceptin block with HER2-Apt-AuNp injection group showed lower enhancement than the HER2-Apt-AuNp group and AuNp group. The contrast enhancement of tumor for the targeted or non-targeted Lipo-I contrast agent injection groups (Lipo-I, VEGFR-Apt-Lipo-I) was highest immediately after contrast administration in both groups and was decreased at 24 hours (Figures 3 and 5). The contrast enhancement at 48 hours was decreased in the non-targeted imaging group (Lipo-I) but slightly increased in the targeted imaging group (VEGFR-Apt-Lipo-I). The VEGFR-Apt-Lipo-I group demonstrated greater enhancement than the Lipo-I group immediately and 24 and 48 hours after contrast administration.

(a) AuNp group

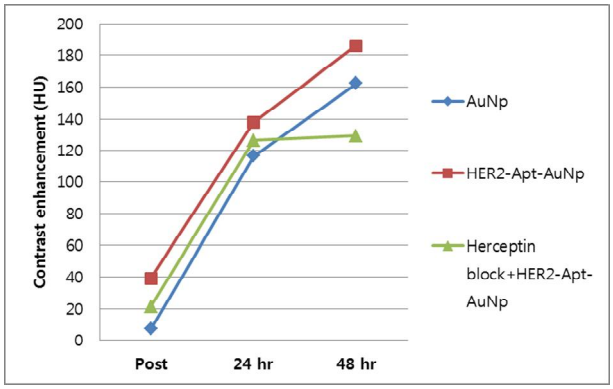

(b) Lipo-I group

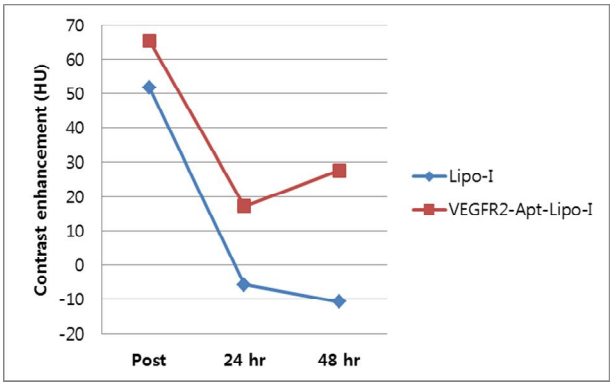

(c) Dual contrast group

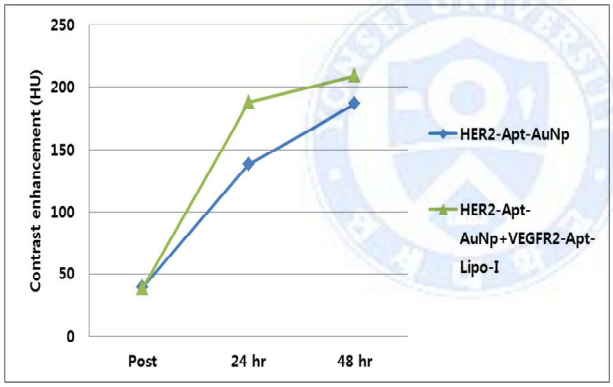

Figure 3. Time-based changes in contrast enhancement of tumor. (a-b) The contrast enhancement of tumor was higher for targeted agent than non-targeted agent. (c) Injection of dual targeted contrast showed higher contrast enhancement than single agent after 24 and 48 hours.

.

(a) HER2-Apt-AuNp

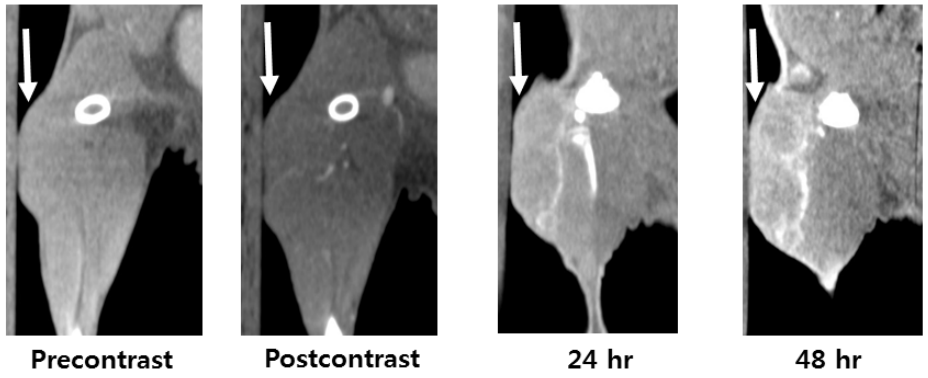

(b) AuNP

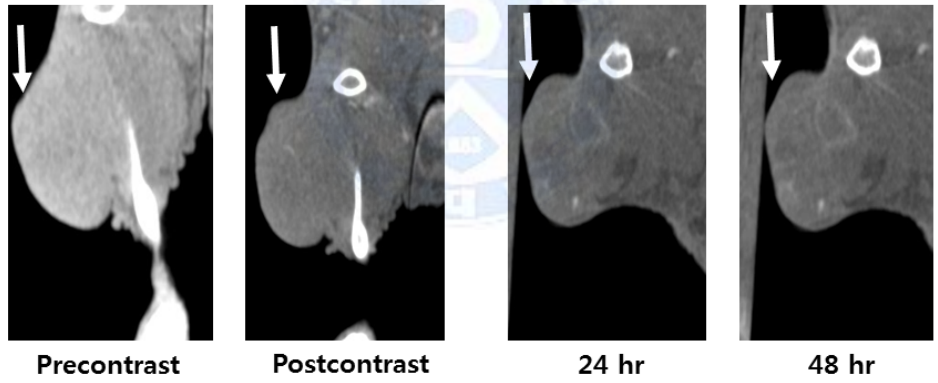

Figure 4. In vivo micro-CT imaging of HER2-Apt-AuNp and AuNp injected into a breast cancer model in BALB/c nude mice. CT images acquired before and immediately, 24 hours, and 48 hours after contrast administration show contrast enhancement within tumor (arrows). Tumor in a mouse injected with HER2-Apt-AuNp (a) showed stronger contrast enhancement than tumor in a mouse injected with AuNp (b).

(a) VEGFR-Apt-Lipo-I

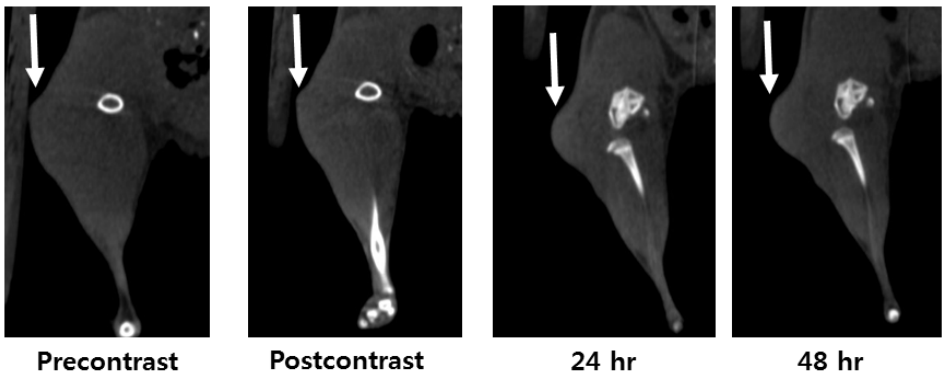

(b) Lipo-I

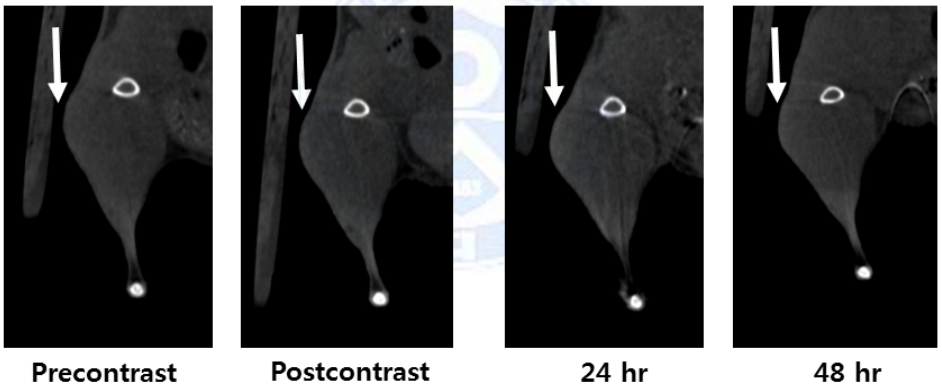

Figure 5. In vivo micro-CT imaging of a tumor model with VEGFR-Apt-Lipo-I and Lipo-I injection. CT images of a mouse injected with VEGFR2-Apt-Lipo-I (a) show contrast enhancement within tumor (arrows), which was greater than that in images from a mouse with Lipo-I injection (b).

3. In vivo imaging: simultaneous imaging acquisition of dual targeting contrast agents

The combination of VEGFR-Apt-Lipo-I with HER2-Apt-AuNp showed less contrast enhancement than HER2-Apt-AuNp alone immediately after contrast injection, but greater contrast enhancement at 24 hours and 48 hours (Figure 3).

4. Correlation between CT image analysis and histology

The area showing contrast enhancement within the tumor in the AuNp groups (AuNp, HER2-Apt-AuNp, Herceptin block with HER2-Apt-AuNp) was consistent with the area of gold uptake on H&E staining, and largely consistent with the HER2-positive area on IHC staining (Figure 6). The area showing contrast enhancement within the tumor in the Lipo-I and VEGFR2-Lipo-I injection groups was partly consistent with the VEGFR2-positive area on IHC staining (Figure 7).

(a) HER2-Apt-AuNp

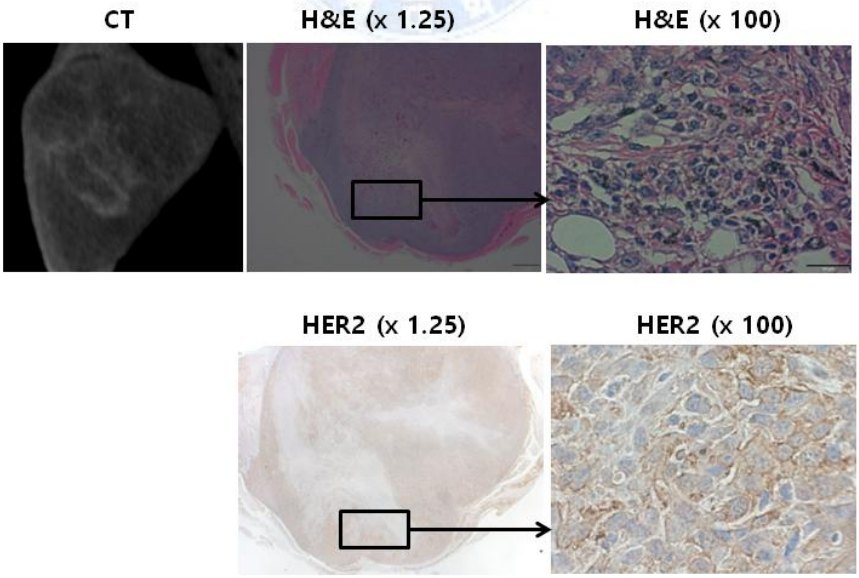

(b) AuNp

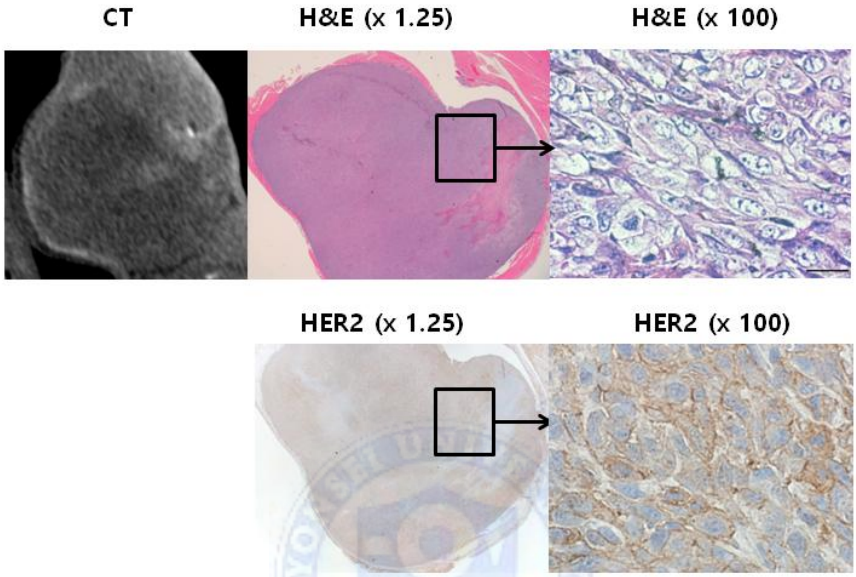

Figure 6. Correlation of CT images with histologic analysis in the AuNp group. Micro-CT images acquired 48 hours after contrast injection show greater contrast enhancement in a mouse injected with HER2-Apt-AuNp (a) than with AuNp (b). On H&E staining, uptake of AuNp seen on both ×1.25 (within box) and ×100 images was largely consistent with the HER2-positive area (within box) on immunohistochemical staining.

(a) VEGFR2-Apt-Lipo-I

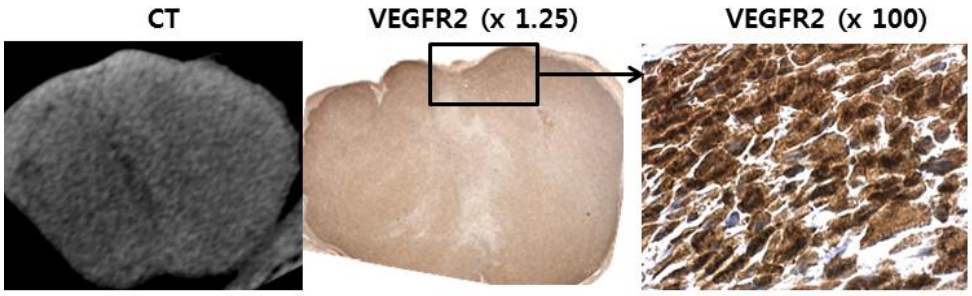

(b) Lipo-I

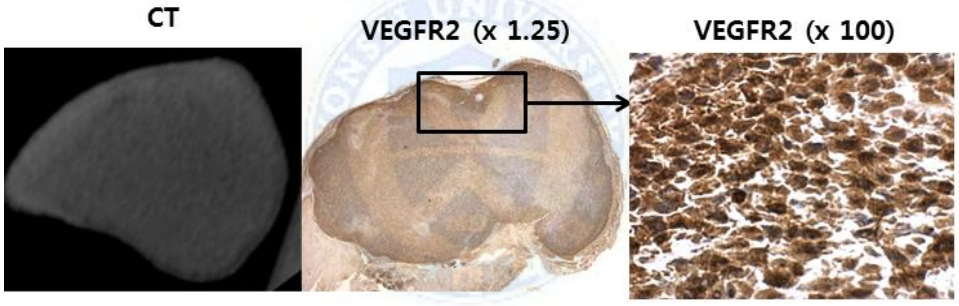

Figure 7. Correlation of CT images with histologic analysis in the Lipo-I group. Micro-CT images acquired 48 hours after contrast injection show greater contrast enhancement in a mouse injected with VEGFR2-Apt-Lipo-I (a) within the area showing VEGFR2-postivity on immunohistochemical staining (within the box) than in a mouse injected with Lipo-I (b).

IV. DISCUSSION

In this study, we established a preclinical micro-CT imaging protocol that allows visualization of targeted nanoparticle contrast agents (HER2-apt-AuNp and VEGFR2-Apt-Lipo-I) in vivo by CT imaging in a mouse breast cancer model. By CT image analysis we could visualize the contrast enhancement for each nanoparticle contrast agent, even with simultaneous administration of two targeted nanoparticles. Moreover, the CT-derived measurements of both nanoparticle contrast agents were correlated with histology and IHC staining.

Simultaneous visualization of two or more different targets in a single tumor is important for the diagnosis and treatment of tumor. Personalized medicine in oncology, such as targeted chemotherapy, has recently been emphasized and has become a mainstream cancer therapy. For example, in breast cancer, the second leading cause of cancer death in women, determination of tumor estrogen receptor, progesterone receptor, and HER2 status before treatment is essential to decide the treatment plan and predict treatment response and prognosis.[16] VEGFR2 expression is thought to be another potentially important marker in breast cancer that contributes to tumor angiogenesis.[17] The combination of trastuzumab (anti-HER2 agent) with bevacizumab (anti-VEGF agent) for breast cancer therapy has shown promising results in preclinical xenograft studies because preadministration of the anti-VEGF agent reduced vascular permeability and blood perfusion and resulted in decreased tumor uptake of trastuzumab.[18] Therefore, we selected HER2 and VEGFR2 as two targets in breast cancer in our study.

Previous studies investigated in vivo CT imaging with nanoparticles as the CT contrast agent, mainly using AuNp and Lipo-I. However, few targeted in vivo CT imaging studies using nanoparticles have been reported. Some studies demonstrated targeted CT imaging in animal tumors[7,14] and atherosclerosis.[8] Most of those studies reported the targeting ability of nanoparticle CT contrast

agent, mainly using AuNp. Hainfield et al. demonstrated that HER2 Ab-targeted 15-nm AuNps showed preferential uptake in human breast tumors in a mouse model, but even untargeted AuNps enhanced the visibility of tumor peripheries and enabled detection of millimeter-sized tumors.[7] Similarly, in our study both HER2-targeted AuNp and non-targeted AuNp showed contrast enhancement within the tumor. However, targeted AuNp showed greater contrast enhancement, which could be explained by the targeting effect of the HER2-aptamer. A commonly observed phenomenon with nanoparticles in vivo is the "enhanced permeability and retention" effect.[19,20] The tumor vasculature is more permeable because of angiogenesis, and nanoparticles tend to leak out and are retained in the tissue. Poor central circulation of carcinomas would account for the predominant accumulation at the growing periphery of the tumor and would also explain why the non-targeted AuNp agent was also accumulated within the tumor, but mainly at the periphery. Penetration into the tumor might be enhanced by using smaller gold particles or an antibody or aptamer. We indirectly proved the targeting effect based on the correlation between CT imaging and IHC staining. Areas of higher contrast enhancement on targeting imaging were largely consistent with HER2- or VEGFR2-positive areas on IHC staining. Moreover, we observed that AuNps without an aptamer had better tumor uptake than those with aptamer and Herceptin block, probably because the effect of targeting on contrast enhancement was abrogated by blocking the target pathway with Herceptin.

Although studies using near-infrared imaging for simultaneous visualization of dual targets have been reported,[21] there are few simultaneous targeting imaging studies with CT. Demonstration of contrast enhancement by two different contrast materials on CT has been reported, mainly using dual-energy or multi-energy techniques.[4,8,22,23] Some investigators demonstrated that dual-energy micro CT enabled the simultaneous quantification of tumor blood volume by AuNp and vascular permeability by Lipo-I on a single scan of

mouse tumor.[4,22] However, our study is the first to investigate the feasibility of simultaneous dual-targeting imaging in animal tumors using CT. Although accurate differentiation and quantification of each contrast material was not possible in our study, our data suggest the feasibility of a simultaneous dual-targeting CT study with the demonstration of different contrast enhancement according to the different combinations of contrast agent. We are convinced that issues of quantification and differentiation will be solved by advanced CT techniques that have the capability of material decomposition, such as multi-energy spectral CT.

Our study has certain limitations. First, the area of contrast enhancement by nanoparticles was largely consistent with the target-positive area on IHC staining. Nevertheless, non-targeting effects such as uptake by macrophages may contribute to contrast enhancement. However, we demonstrated the targeting effect indirectly via the correlation with IHC staining and Herceptin blocking. Second, quantification and differentiation of each nanocontrast material was not feasible in this study. Advanced CT techniques such as dual-energy or multi-energy CT allow selective visualization and quantification of contrast agents and show high promise in the clinic for cancer imaging.[3,4,22,24] We suggest that further studies with multi-energy micro-CT will solve the problems regarding material differentiation and quantification.

V. CONCLUSION

Micro-CT can be applicable for simultaneous in vivo imaging of dual tumor targets. However, for differentiation and quantification of enhancement by each nanoprobe, further studies with advanced CT techniques such as multi-energy spectral CT will be needed.

REFERENCES

1. Ke S, Wang W, Qiu X, Zhang F, Yustein JT, Cameron AG, et al. Multiple target-specific molecular agents for detection and image analysis of breast cancer characteristics in mice. Curr Mol Med 2013;13:446-58.
2. Li PC, Wang CR, Shieh DB, Wei CW, Liao CK, Poe C, et al. In vivo photoacoustic molecular imaging with simultaneous multiple selective targeting using antibody-conjugated gold nanorods. Opt Express 2008;16:18605-15.
3. Clark DP, Ghaghada K, Moding EJ, Kirsch DG, Badea CT. In vivo characterization of tumor vasculature using iodine and gold nanoparticles and dual energy micro-CT. Phys Med Biol 2013;58:1683-704.
4. Ashton JR, Clark DP, Moding EJ, Ghaghada K, Kirsch DG, West JL, et al. Dual-Energy Micro-CT Functional Imaging of Primary Lung Cancer in Mice Using Gold and Iodine Nanoparticle Contrast Agents: A Validation Study. PLoS One 2014;9:e88129.
5. Au JT, Craig G, Longo V, Zanzonico P, Mason M, Fong Y, et al. Gold nanoparticles provide bright long-lasting vascular contrast for CT imaging. AJR Am J Roentgenol 2013;200:1347-51.
6. Danila D, Johnson E, Kee P. CT imaging of myocardial scars with collagen-targeting gold nanoparticles. Nanomedicine 2013;9:1067-76.
7. Hainfeld JF, O'Connor MJ, Dilmanian FA, Slatkin DN, Adams DJ, Smilowitz HM. Micro-CT enables microlocalisation and quantification of Her2-targeted gold nanoparticles within tumour regions. Br J Radiol 2011;84:526-33.
8. Cormode DP, Roessl E, Thran A, Skajaa T, Gordon RE, Schlomka JP, et al. Atherosclerotic plaque composition: analysis with multicolor CT and targeted gold nanoparticles. Radiology 2010;256:774-82.
9. Aydogan B, Li J, Rajh T, Chaudhary A, Chmura SJ, Pelizzari C, et al. AuNP-DG: deoxyglucose-labeled gold nanoparticles as X-ray computed

tomography contrast agents for cancer imaging. Mol Imaging Biol 2010;12:463-7.

10. Cai QY, Kim SH, Choi KS, Kim SY, Byun SJ, Kim KW, et al. Colloidal gold nanoparticles as a blood-pool contrast agent for X-ray computed tomography in mice. Invest Radiol 2007;42:797-806.

11. Peng C, Li K, Cao X, Xiao T, Hou W, Zheng L, et al. Facile formation of dendrimer-stabilized gold nanoparticles modified with diatrizoic acid for enhanced computed tomography imaging applications. Nanoscale 2012;4:6768-78.

12. Peng C, Zheng L, Chen Q, Shen M, Guo R, Wang H, et al. PEGylated dendrimer-entrapped gold nanoparticles for in vivo blood pool and tumor imaging by computed tomography. Biomaterials 2012;33:1107-19.

13. Wang H, Zheng L, Peng C, Guo R, Shen M, Shi X, et al. Computed tomography imaging of cancer cells using acetylated dendrimer-entrapped gold nanoparticles. Biomaterials 2011;32:2979-88.

14. Liu H, Xu Y, Wen S, Chen Q, Zheng L, Shen M, et al. Targeted tumor computed tomography imaging using low-generation dendrimer-stabilized gold nanoparticles. Chemistry 2013;19:6409-16.

15. Lee H, Lee K, Kim IK, Park TG. Fluorescent Gold Nanoprobe Sensitive to Intracellular Reactive Oxygen Species. Advanced Functional Materials 2009;19:1884-90.

16. Gradishar WJ, Anderson BO, Blair SL, Burstein HJ, Cyr A, Elias AD, et al. Breast cancer version 3.2014. J Natl Compr Canc Netw 2014;12:542-90.

17. Pegram MD, Reese DM. Combined biological therapy of breast cancer using monoclonal antibodies directed against HER2/neu protein and vascular endothelial growth factor. Semin Oncol 2002;29:29-37.

18. Pastuskovas CV, Mundo EE, Williams SP, Nayak TK, Ho J, Ulufatu S, et al. Effects of anti-VEGF on pharmacokinetics, biodistribution, and tumor penetration of trastuzumab in a preclinical breast cancer model. Mol Cancer

Ther 2012;11:752-62.

19. Noguchi Y, Wu J, Duncan R, Strohalm J, Ulbrich K, Akaike T, et al. Early phase tumor accumulation of macromolecules: a great difference in clearance rate between tumor and normal tissues. Jpn J Cancer Res 1998;89:307-14.

20. Dvorak HF, Nagy JA, Dvorak JT, Dvorak AM. Identification and characterization of the blood vessels of solid tumors that are leaky to circulating macromolecules. Am J Pathol 1988;133:95-109.

21. Sun Y, Shukla G, Pero SC, Currier E, Sholler G, Krag D. Single tumor imaging with multiple antibodies targeting different antigens. Biotechniques 2012;52.

22. Moding EJ, Clark DP, Qi Y, Li Y, Ma Y, Ghaghada K, et al. Dual-energy micro-computed tomography imaging of radiation-induced vascular changes in primary mouse sarcomas. Int J Radiat Oncol Biol Phys 2013;85:1353-9.

23. Anderson NG, Butler AP, Scott NJ, Cook NJ, Butzer JS, Schleich N, et al. Spectroscopic (multi-energy) CT distinguishes iodine and barium contrast material in MICE. Eur Radiol 2010;20:2126-34.

24. Badea CT, Guo X, Clark D, Johnston SM, Marshall CD, Piantadosi CA. Dual-energy micro-CT of the rodent lung. Am J Physiol Lung Cell Mol Physiol 2012;302:L1088-97.

ABSTRACT(IN KOREAN)

종양 이중 표적의 생체 동시 영상: 이중 조영 나노프로브와 컴퓨터단층촬영을 이용한 발견과 정량화

<지도교수 허 진>

연세대학교 대학원 의학과

서 영 주

배경: 종양의 진단에서 다중 표적자의 사용은 정확한 진단과 개인별맞춤 치료를 가능하게 하여 점차 표준적 임상 진료 방법이 되고 있다. 본 연구는 종양 내 발현하는 이중 표적을 이중 조영제 및 마이크로 전산화 단층 촬영을 이용하여 동시 영상화하는 것을 목적으로 하였다.

방법: Polyethylene glycol 로 싸여진 30nm 크기의 금 나노조영제를 Her2 압타머와 결합시키고, 리포좀으로 싸여진 요오드 조영제를 VEGFR2 압타머와 결합하여 표적 나노조영제를 합성하였다. HER2 가 고발현하는 종양모델을 만들어 암컷 BALB/c-nude mice 에 이식하여 동물 모델을 준비하였다. 금과 요오드의 표적, 비표적 나노조영제를 각각 정맥 주입하여 마이크로 컴퓨터 전산화 단층 촬영 영상을 획득하였다. 종양 내의 컴퓨터 전산화 단층 촬영에서의 조영 정도를 측정하여 조영제 주입 군 간에 비교하였다. 컴퓨터 전산화 단층 촬영에서의 측정값을 조직학적 염색 결과와 비교하였다.

결과: 종양 내 조영 증강 정도는 HER2-Apt-AuNp 군에서 AuNp 군보다 높았다 (조영제 주입 직후: 39.4 대 7 HU, 24 시간 후 138.1 대

116.6 HU), 48 시간 후 186.0 대 162.4 HU). Herceptin block 을 시행한 후 HER2-Apt-AuNp 주입한 군은 HER2-Apt-AuNp 군과 AuNp 군보다 모두 낮은 조영 증강 정도를 보였다 (조영제 주입 48시간 후 조영 증강 129.2 HU). VEGFR-Apt-Lipo-I 군은 Lipo-I 군보다 높은 조영 증강 정도를 보였다 (조영제 주입 직후 조영 증강 65.4 HU 대 51.8 HU). VEGFR-Apt-Lipo-I 와 HER2-Apt-AuNp 를 동시 주입한 군은 HER2-Apt-AuNp 단독 주입군보다 높은 조영 증강을 보였다 (조영제 주입 24 시간 후 187.4 대 138.1 HU, 48 시간 후 208.5 대 186 HU). 종양내 금 또는 리포좀화 요오드에 의해 조영 증강을 보이는 구역은 면역조직화학염색에서 HER2 양성 혹은 VEGFR2 양성인 부분과 부분적으로 일치하였다.

결론: 마이크로 컴퓨터전산화 단층촬영은 생체 내 이중 표적의 동시 영상화에 활용 가능한 방법이다.

핵심되는 말: 컴퓨터 전산화 단층 촬영, 표적 영상, 이중 나노 조영제